Isomeric Co(II) paraCEST agents as pH responsive MRI probes

Journal:	*Dalton Transactions*
Manuscript ID	DT-COM-11-2019-004558
Article Type:	Communication
Date Submitted by the Author:	27-Nov-2019
Complete List of Authors:	Bond, Christopher; University at Buffalo, SUNY, chemistry Cineus, Roy; University at Buffalo, SUNY, chemistry Nazarenko, Alexander; State University of New York College at Buffalo, Chemistry Spernyak, Joseph; Roswell Park Cancer Institute, Department of Cell Stress Biology Morrow, Janet; University at Buffalo, SUNY, chemistry

Isomeric Co(II) paraCEST agents as pH responsive MRI probes

Christopher J. Bond,[a] Roy Cineus,[a] Alexander Y. Nazarenko,[b] Joseph A. Spernyak[c] and Janet R. Morrow[a*]

[a]Department of Chemistry, Natural Sciences Complex, University at Buffalo, the State University of New York, Amherst, NY 14260

[b]Chemistry Department, SUNY College at Buffalo, 1300 Elmwood Ave, Buffalo, NY 14222

[c]Department of Cell Stress Biology, Roswell Park Comprehensive Cancer Institute, Buffalo, NY 14263

*corresponding author at jmorrow@buffalo.edu

Abstract

A newly discovered isomer of Co(II) (1,4,8,11-tetrakis(carbamoylmethyl)-1,4,8,11-tetraazacyclotetradecane = CCRM) produces four highly paramagnetically shifted chemical exchange saturation transfer (CEST) peaks. The 1,8-pendants of the complex are bound in a trans-arrangement to produce a Co(II) complex of increased kinetic inertness.   The isomers have a stabilized Co(II) center ($E_{1/2}$ of 540 to 550 mV versus SHE).   Both the 1,8 and the 1,4-isomer are excellent pH probes in solution and in tissue homogenate by virtue of their highly paramagnetically shifted amide protons. These isomers produce both a ratiometric pH readout as well as amide proton exchange rate constants that correlate to pH.

Introduction

The development of MRI contrast agents that register changes in biological environment through modulation of the proton water signal is of great interest to researchers in the field of molecular imaging.[1]   MRI has the high resolution and good depth penetration needed for such in vivo studies. Contrast agents are used to improve images, and are frequently used for the detection of tumors and lesions. Responsive MRI probes may have additional properties that enable tracking of changes in pH,[2-3] temperature,[4] or redox[5] in tissue. Of special interest to the characterization of disease states is monitoring changes in pH.[2] For example, a correlation between acidic extracellular pH and metastatic tumor aggressiveness has been postulated[6] and there has been much effort to develop responsive pH probes for assessment of tumors.[3]

One approach to pH responsive probes features paramagnetic transition metal ion complexes that produce contrast through chemical exchange saturation transfer (CEST or paraCEST).[7] To produce the CEST signal, paramagnetically shifted proton resonances of the transition metal complex are magnetically saturated upon irradiation with a radiofrequency pulse and, upon exchange with bulk water protons, produce a decrease in the intensity of the water signal. A plot of the intensity of the water proton resonance as a function of the radiofrequency pulse (Z-spectrum) shows CEST peaks for the exchangeable protons. Typically, the rate constants for proton exchange and the corresponding intensity of the CEST peaks vary with pH. This suggests the possibility of using relative intensities of CEST peaks to register pH for agents that have different types of exchangeable protons.[8-9]

Divalent Co(II), Ni(II) and Fe(II) complexes form paraCEST agents with pH,[8, 10-11] temperature,[12-13] or redox[14] responsive properties. Our focus has been on macrocyclic complexes, which are inert towards dissociation under biologically relevant conditions. One particularly interesting series of macrocyclic complexes contains the 1,4,8,11-tetrakis(carboamoylmethyl)-1,4,8,11 tetraazacyclotetradecane (CCRM) ligand and either Fe(II), Co(II) or Ni(II).[10, 12, 15] The Co(II) complex, $[Co(1,4-CCRM)]^{2+}$, is a paraCEST agent that produces four distinct CEST peaks, all with strong intensity, and with the furthest shifted

CEST peak at 112 ppm versus bulk water at 37 °C and pH 7.3-7.5.[10] A disadvantage of the complex is its low kinetic inertness towards dissociation, so it was of interest to design analogs that are more robust. Here we show that a coordination isomer with bound amide pendents in the 1 and 8 positions on the ring ([Co(1,8-CCRM)]$^{2+}$) is substantially more inert towards dissociation than the original isomer, opening up new opportunities to design paraCEST agents based on the cyclam framework (Scheme 1). Studies at both high and moderate magnetic field strengths in solution and tissue homogenate are promising for the development of pH responsive MRI contrast agents.

Scheme 1: Synthesis and isomerization of [Co(CCRM)]Cl$_2$ complexes.
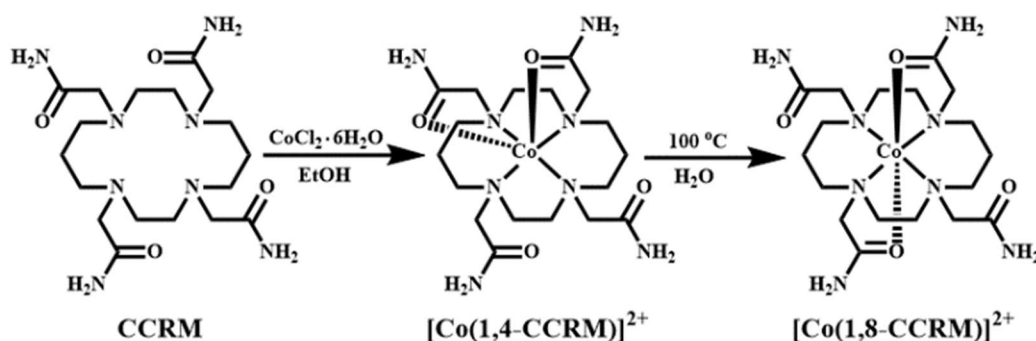
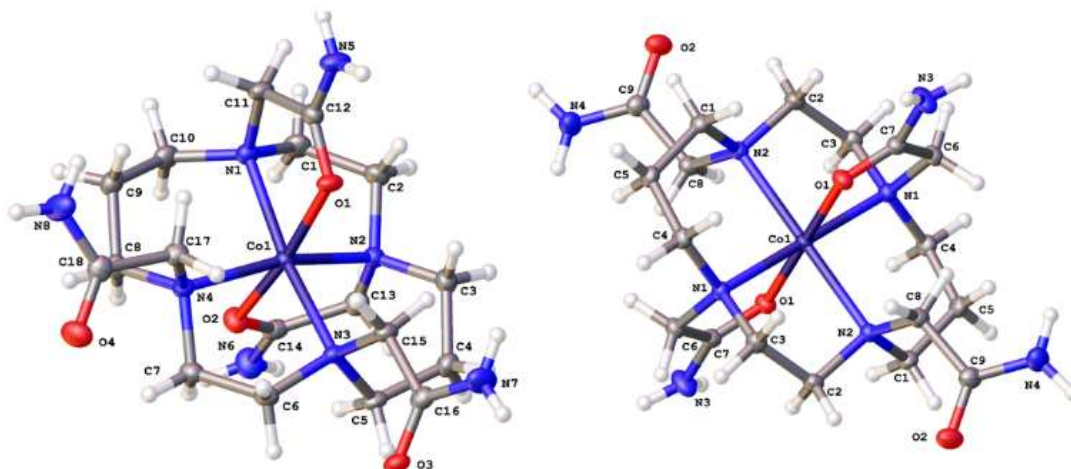Figure 1. Crystals structures of the complex cations of [Co(1,4-CCRM)][Co(NCS)$_4$] (left) and [Co(1,8-CCRM)](NCS)$_2$ (right).   Counterions were excluded for clarity. Crystal data, and structure refinement is summarized in Table S1.

Results and Discussion

The two different isomers of [Co(CCRM)]$^{2+}$ were characterized in the solid state. The complexes were crystalized from two solutions, one that was kept at room temperature and one that was heated for two hours at 100°C in water, before being cooled and allowed to crystallize. The crystal structure in Figure 1 (left) was produced from the sample that was not exposed to heat, and matches the 1,4-coordination isomer of the previously published structure.[10, 12] The crystal structure of the complex as shown in Figure 1 (right) was obtained from the solution exposed to heat, and displays a 1,8-coordination isomer. In addition to the differences in pendent group binding, there was a change in the macrocyclic ring conformation from a trans-R,R,R,S in the 1,4-isomer to a trans-S,S,R,R, for the 1,8-isomer, where R and S refer to the stereochemistry around the ring nitrogen atoms. Notably, the trans-SSRR structure is the most stable for divalent transition metal complexes.[16-18]

Proton NMR studies are consistent with the formation of [Co(1,8-CCRM)]$^{2+}$ and the disappearance of most of the [Co(1,4-CCRM)]$^{2+}$ upon heating the solution (Figure S1). The ^{1}H NMR spectrum of [Co(1,4-CCRM)]$^{2+}$ contained 25 peaks between 260 and -75 ppm,

with one peak having double the integration of the others, indicating a total of 26 inequivalent paramagnetically shifted proton resonances, as expected for nonexchangeable protons of the CCRM complex, (Figure S2A). Heating the sample in D_2O lead to a ^{1}H NMR spectrum with 20 new significant resonances between 290 and -140 ppm (Figure S2B), consistent with isomerization but corresponding to fewer resonances than expected. Indeed, heating $[Co(1,4-CCRM)]^{2+}$ in H_2O, followed by removal of H_2O and then dissolution of the residue in D_2O, produced an additional 6 proton resonances, suggesting that the methylene protons adjacent to amides exchange with deuterium at high temperature (Figure S2C).

The ^{1}H NMR spectrum of the new complex was maintained over several days at room temperature with no sign of converting back to the original isomer. These data are consistent with the temperature driven isomerization of the $[Co(1,4-CCRM)]^{2+}$ complex to $[Co(1,8-CCRM)]^{2+}$. Notably, we could not completely convert the 1,4- isomer to the 1,8-isomer. The ratio reached was approximately 15:85 of 1,4-isomer to 1,8-isomer after boiling the sample in water for several hours. Mass spectra (Figure S3) of solutions containing complex before and after heating in water showed identical spectra for the complexes. The magnetic moment of samples, as determined by using Evans method[19-20] at 25°C were similar (μ_{eff} = 4.6 and 4.7) for the complexes before and after heating.

The kinetic inertness of the new isomer was studied under several conditions including acid or biological anions (HCO_3^{2-}, HPO_4^{3-}), or with competing Zn^{2+} or Cu^{2+} ions, and compared with studies on $[Co(1,4-CCRM)]^{2+}$ (Table S2). This data shows that $[Co(1,8-CCRM)]^{2+}$ is more inert than $[Co(1,4-CCRM)]^{2+}$, especially when incubated in acid (pD 3.5-4) for 12 hours at 37 °C, with little dissociation of $[Co(1,8-CCRM)]^{2+}$ (Figure S4), compared to 95% of Co(1,4-CCRM).[10] Both complexes were stable in the presence of biologically relevant anions. In the presence of equimolar Cu^{2+} ion, $[Co(1,4-CCRM)]^{2+}$ almost completely dissociates (93%) after 5 hours, but $[Co(1,8-CCRM)]^{2+}$ shows little dissociation over the same time period (Figure S7 and Table S3). That $[Co(1,8-CCRM)]^{2+}$ is more resistant to dissociation corroborates its assignment as the thermodynamically favored

isomer, whereas [Co(1,4-CCRM)]$^{2+}$ is the kinetically favored form produced at lower temperatures.

The two complexes were also stable towards oxidation to Co(III). Cyclic voltammetry studies in aqueous solution at neutral pH, 100 mM KCl showed electrochemistry consistent with quasi-reversible redox processes with an E$_{1/2}$ of 540 and 550 mV versus SHE for [Co(1,4-CCRM)]$^{2+}$ and [Co(1,8-CCRM)]$^{2+}$, respectively (Figure S8). Likewise, electronic spectra of the two complexes were similar with peak maxima at close to 490 nm and low extinction coefficients (12 and 18 M^{-1}cm^{-1}) representative of d-d transitions (Figs S9, S10).
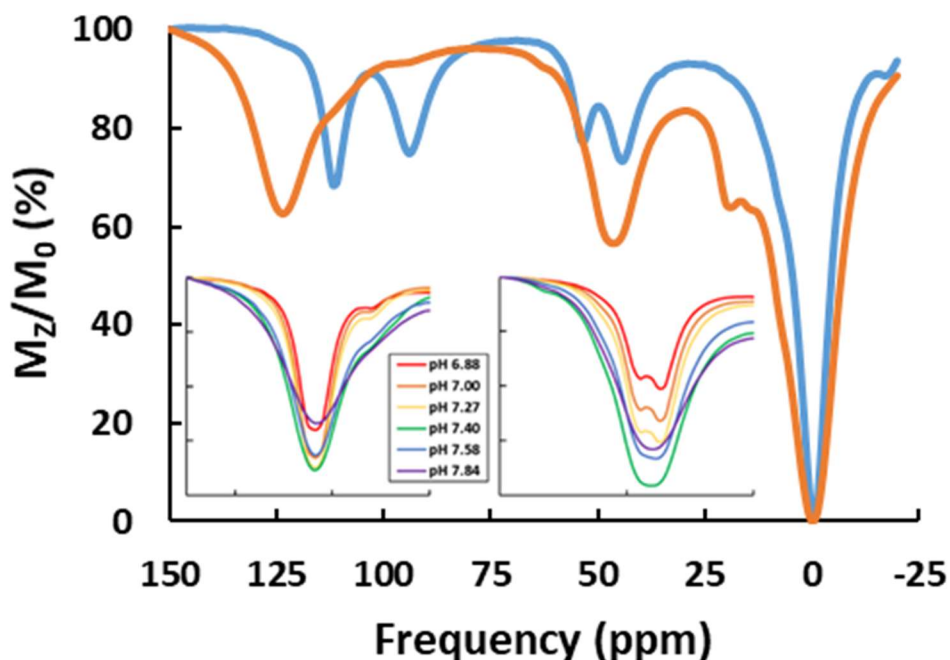

Figure 2. Z-spectra taken at 37°C of [Co(CCRM)]$^{2+}$ before (1,4-isomer, blue) and after(1,8-isomer, orange) heating with B$_1$ = 29 μT at 11.7 T. The sample contained 10mM complex, 20 mM pH 7.40 HEPES buffer, and 100 mM NaCl. The inset features overlays of the 1,8-isomer at pH values between 6.88 and 7.84.

Two intense CEST peaks were observed for [Co(1,8-CCRM)]$^{2+}$ at 37 ^{o}C and pH 7.4, shifted 124 ppm and 45 ppm away from bulk water, with intensities of 35 $\pm$ 2 % and 38 $\pm$

1 % CEST respectively (Figure 2). Note that under the same conditions and at the same concentration, the CEST peaks for $[Co(1,8\text{-}CCRM)]^{2+}$ are more intense and further shifted than the previously studied $[Co(1,4\text{-}CCRM)]^{2+}$ complex. Z spectra taken with a reduced saturation power (12.7 µT) resulted in narrower CEST peaks, allowing for overlapping peaks to be distinguished (Figure S11) for a total of four highly shifted CEST peaks assigned to the four distinct bound amide protons. Small peaks in the $[Co(1,8\text{-}CCRM)]^{2+}$ CEST spectra also indicate a low concentration of the 1,4-isomer, just as we observed in the NMR spectra. In addition, there are four CEST peaks in the range of 7 ppm to 20 ppm versus water that are assigned to the amide NH protons of the uncoordinated pendents.

CEST peak intensity of the amide protons is pH sensitive, consistent with reports of other amide based CEST agents.[8, 10, 21-22] Figure 3 (left) shows the intensity of the $[Co(1,8\text{-}CCRM)]^{2+}$ CEST peaks at 124 and 45 ppm respectively. The exchange rate constants as calculated by using the HW-Quesp[23] methods (Table S4) are consistent with an increase in rate constants with pH as promoted by base catalyzed exchange. The k_{ex} increases with respect to increasing pH values until the exchange broadening produces an overall decrease in the CEST peak intensity, above pH 7.4 in the case of $[Co(1,8\text{-}CCRM)]^{2+}$. The saturation transfer (ST) values are used to calculate the ratio of the CEST intensity at each pH value. Over the pH range of the experiments, the data is linear as shown in Figure 3 (right). Experiments were also run at the lower pulse power of 12.7 µT (Figures S11 and S12) which is suitable for animal experiments.[24] The experiments carried out at the lower power of 12.7 µT gave four resolved CEST peaks and allowed us to take the ratio of the two most intense of the four peaks. A plot of the pH dependence of the peaks at this lowered power gave a slightly lower slope of 0.26 (Figure S12).

A complicating feature of CEST peak position and intensity is their strong temperature dependence. As shown in Figure S13, temperature has a strong effect on most highly shifted CEST peaks in particular. The far shifted CEST peak at 125 ppm shifts more positive by 0.61 ppm per degree. The intensity of the CEST peak changes with temperature as well. This data shows that a concurrent change in temperature may complicate the analysis of pH. The strong temperature dependence of the CEST peaks is

a particular concern for application of paraCEST agents in anesthetized animals where the temperature may fluctuate.
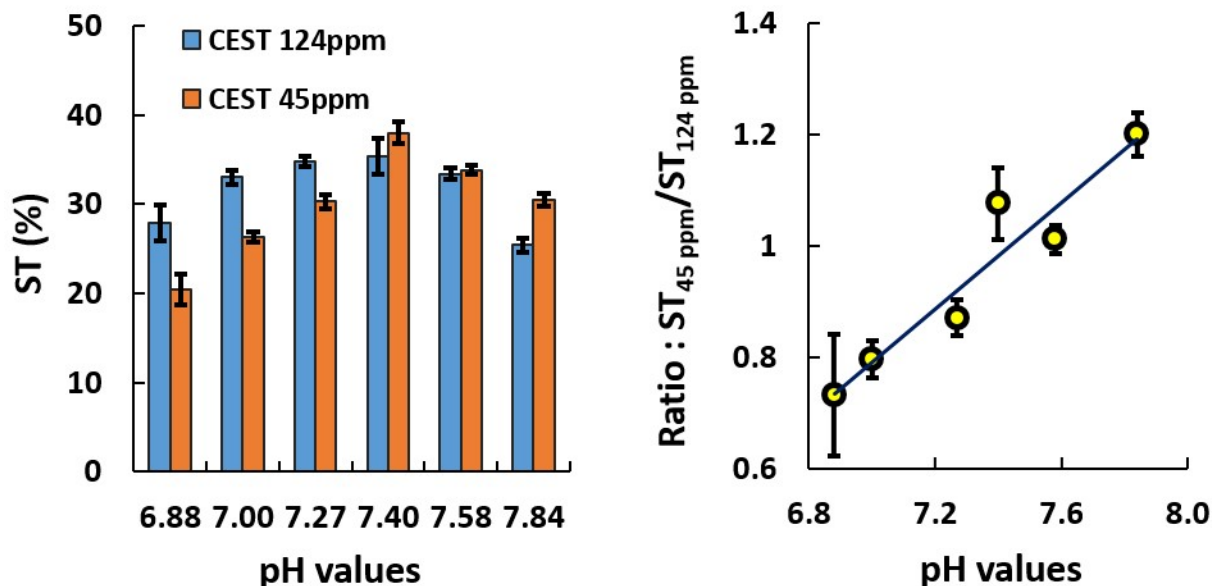

Figure 3: The saturation transfer (ST= (1-M_Z/M_0) x100) is graphed at each pH (left), and the ratio of the CEST peaks (45ppm/124ppm) at a given pH value is plotted (right), and fit to a line with a slope of 0.48 and R^2=0.91 at 11.7 T. Presaturation pulse power, B_1 = 29 μT.

Phantom imaging on a 4.7 T small animal MRI scanner was studied to investigate the effect of lower magnetic field strength on pH mapping by the new Co(II) paraCEST agent. Samples contained 10 mM Co(II) complex, with pH values between 6.6 and 7.8 at 37 °C. The relative intensities of CEST peaks at 44 ppm and 124 ppm were plotted as a function of pH, and the pH ratio of the CEST peak intensities showed linearity between pH values of 6.6 and 7.8 (Figure S15). Notably, the slope in this ratiometric experiment is nearly double that recorded on the 11.7 T NMR spectrometer. Differences in slope are attributed in part to the overlapping pairs of CEST peaks that are resolved at 11.7 T but not on the 4.7 T MRI scanner as well as the larger inherent error in measurements made

on the MRI scanner as shown by error bars in the graph. The marked difference in Co(II) paraCEST agent peak shape on a high field NMR compared to the lower field MRI scanner used here was compared in our previous studies.[12] The lower pulse power of 12 µT used on the scanner may also affect the slope in the ratiometric pH analysis. However, one set of experiments on the 11.7 T NMR spectrometer with a pulse power (B_1) of 12.7 µT still gave a lower slope than observed on the MRI (Figure S12). This highlights the need to carry out calibration of the pH probe on each instrument.

Various media have been used in the past to simulate tissue in paraCEST studies including agarose and polymerized albumin.[22] Here we recorded Z-spectra of [Co(1,4-CCRM)]$^{2+}$ and [Co(1,8-CCRM)]$^{2+}$ soaked tissue homogenate to simulate the magnetization transfer (MT) effect and to determine whether proteins or other macromolecules in the tissue would affect amide proton exchange and the corresponding pH measurement (Figures 4, S16-17). Chicken thigh meat was incubated for 48 hours with solutions containing 55-60 mM complex at 4°C, then rinsed and ground up into fine pieces. Analysis of the tissue by ICP-MS showed that the concentration of complex in tissue corresponded to 14±1 mM. The Z-spectra show the most highly shifted CEST peaks are easily detectable, while the less highly shifted peaks are obscured by the MT-effect. As expected, the MT effect becomes more problematic at a lower field strength (9.4 T, Fig S15).[25] In these studies, the [Co(1,4-CCRM)]$^{2+}$ isomer which has two highly shifted CEST peaks has an advantage over the [Co(1,8-CCRM)]$^{2+}$ isomer.
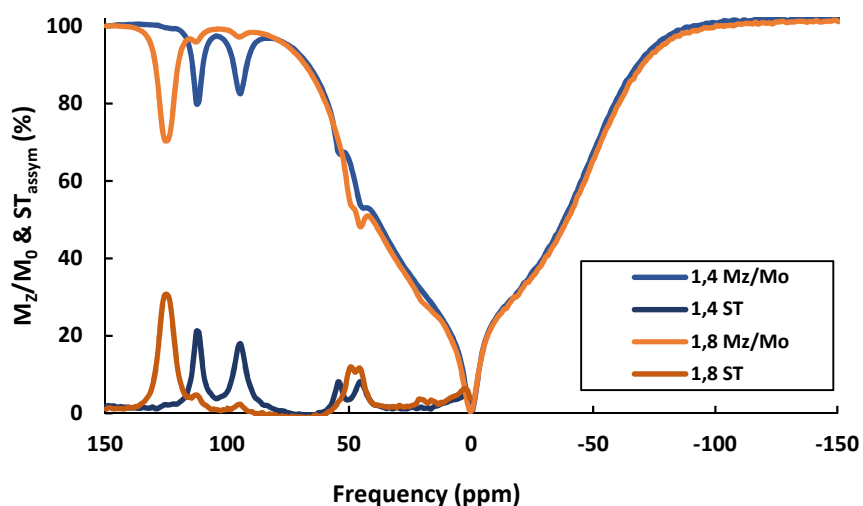
Figure 4: Overlaid Z-spectra and corresponding CEST of the 1,4 and 1,8 complexes incubated in chicken thigh homogenate at 37˚C, B_1 = 12.4 μT at 11.4 T and % CEST= (% ST_{neg} − % St_{pos}). Samples had 14 mM Co(II) complex with a pH of 7.4.

Finally, we studied the CEST effect of the two isomers in the tissue homogenate to further test the complexes as pH probes. In these experiments, we checked the ratio of two CEST peaks and also the proton exchange rate constants of the Co(II) complexes in the tissue, which correlate to pH. The pH of the tissue was 7.4 as measured by a glass electrode. For the 1,4-complex, the ratiometric and exchange rate constants corresponded well with the pH (Figure S20), indicating values of 7.3 and 7.4, respectively. pH mapping with the 1,8-isomer was not feasible by ratiometric analysis as the peak at 45 ppm was obscured by the MT-effect. However, the exchange rate constant at 125 ppm corresponded to a pH value of 7.5 (Figures S20, S21). This correlation is remarkable given the high concentration of proteins and macromolecules in the chicken homogenate that might have affected the proton exchange rate constant of the Co(II) amide protons. Studies of in vivo ratiometric pH measurements with lanthanide agents have shown a 0.5 pH deviation between measured pH and the pH as determined by a ratiometric calibration curve.[26] Improved ratiometric paraCEST agents with a steeper slope for calibrating pH

based on Co(II) complexes have recently been reported, but only in solution NMR studies.[27]

A further consideration for in vivo studies is the requirement of very high aqueous solubility.[26] Solutions of the [Co(1,8-CCRM)]$^{2+}$ complex could be prepared at 40 mM in phosphate saline buffer for a dose of 0.40 mmol/kg in a mouse. This is at the lower dose limit as shown by studies using a lanthanide paraCEST agents for mapping pH in the bladder of mice.[26] Fortunately, further functionalization the [Co(1,8-CCRM)]$^{2+}$ complex to obtain the higher concentrations that are necessary for in vivo studies is feasible through the 4,11-positions. The ancillary pendents, however, must be carefully chosen so that the trans-isomer of the complex is retained. Future work will focus on these derivatives.

Conclusion

In summary, the [Co(1,8-CCRM)]$^{2+}$ complex is the thermodynamically favored isomer which has the advantage of being robust towards dissociation or trans-metalation in comparison to the [Co(1,4-CCRM)]$^{2+}$ complex, as the kinetic isomer. The 1,8-isomer has two very strong CEST peaks consisting of two sets of overlapping NH amide CEST peaks. However, the overlap of the NH CEST peaks makes the ratiometric analysis of peaks strongly dependent both on field strength and on pulse power. Further, the closer proximity of one set of CEST peaks to the bulk water resonance is a disadvantage due to the tissue magnetization transfer effect as shown here. The amide proton exchange rate constant proved to be a remarkably reliable measure of pH, similar to an approach used for diamagnetic CEST agents and despite the likely interaction of macromolecules in the tissue homogenate with the paraCEST agent.[2]


Conflicts of interest

  "There are no conflicts to declare".

Notes and references

1.   Sherry, A. D.; Woods, M., Chemical exchange saturation transfer contrast agents for magnetic resonance imaging. *Annu Rev Biomed Eng* **2008,** *10*, 391-411.

2.   Pavuluri, K.; McMahon, M. T., pH Imaging Using Chemical Exchange Saturation Transfer (CEST) MRI. *Isr J Chem* **2017,** *57* (9), 862-879.

3.   Ferrauto, G.; Castelli, D. D.; Terreno, E.; Aime, S., In vivo MRI visualization of different cell populations labeled with PARACEST agents. *Magn. Reson Med* **2013,** *69* (6), 1703-1711.

4.   Coman, D.; Trubel, H. K.; Rycyna, R. E.; Hyder, F., Brain temperature and pH measured by (1)H chemical shift imaging of a thulium agent. *NMR Biomed* **2009,** *22* (2), 229-239.

5.   Wang, H.; Jordan, V. C.; Ramsay, I. A.; Sojoodi, M.; Fuchs, B. C.; Tanabe, K. K.; Caravan, P.; Gale, E. M., Molecular Magnetic Resonance Imaging Using a Redox-Active Iron Complex. *J Am Chem Soc* **2019,** *141* (14), 5916-5925.

6.   Webb, B. A.; Chimenti, M.; Jacobson, M. P.; Barber, D. L., Dysregulated pH: a perfect storm for cancer progression. *Nat Rev Cancer* **2011,** *11* (9), 671-677.

7.   Zhang, S. R.; Merritt, M.; Woessner, D. E.; Lenkinski, R. E.; Sherry, A. D., PARACEST agents: Modulating MRI contrast via water proton exchange. *Acc Chem Res* **2003,** *36* (10), 783-790.

8.   Thorarinsdottir, A. E.; Du, K.; Collins, J. H. P.; Harris, T. D., Ratiometric pH Imaging with a Co-2(II) MRI Probe via CEST Effects of Opposing pH Dependences. *J Am Chem Soc* **2017,** *139* (44), 15836-15847.

9.   Srivastava, K.; Ferrauto, G.; Young, V. G., Jr.; Aime, S.; Pierre, V. C., Eight-Coordinate, Stable Fe(II) Complex as a Dual (19)F and CEST Contrast Agent for Ratiometric pH Imaging. *Inorg Chem* **2017,** *56* (20), 12206-12213.

10.   Dorazio, S. J.; Olatunde, A. O.; Spernyak, J. A.; Morrow, J. R., CoCEST: cobalt(II) amide-appended paraCEST MRI contrast agents. *Chem Commun* **2013,** *49* (85), 10025-10027.

11.   Tsitovich, P. B.; Cox, J. M.; Spernyak, J. A.; Morrow, J. R., Gear Up for a pH Shift: A Responsive Iron(II) 2-Amino-6-picolylAppended Macrocyclic paraCEST Agent That Protonates at a Pendent Group. *Inorg Chem* **2016,** *55* (22), 12001-12010.

12.   Olatunde, A. O.; Bond, C. J.; Dorazio, S. J.; Cox, J. M.; Benedict, J. B.; Daddario, M. D.; Spernyak, J. A.; Morrow, J. R., Six, Seven or Eight Coordinate Fe-II, Co-II or Ni-II Complexes of Amide-Appended Tetraazamacrocycles for ParaCEST Thermometry. *Chem-Eur J* **2015,** *21* (50), 18290-18300.

13.   Jeon, I. R.; Gaudette, A. I.; Park, J. G.; Haney, C. R.; Harris, T. D., Spin crossover iron(II) complexes as PARACEST MRI thermometers.   *Chem Sci* **2014,** 5, 2461-2465.

14.   Tsitovich, P. B.; Spernyak, J. A.; Morrow, J. R., A Redox-Activated MRI Contrast Agent that Switches Between Paramagnetic and Diamagnetic States. *Angew Chem Int Edit* **2013,** *52* (52), 13997-14000.

15.   Olatunde, A. O.; Dorazio, S. J.; Spernyak, J. A.; Morrow, J. R., The NiCEST Approach: Nickel(II) ParaCEST MRI Contrast Agents. *J. Am Chem Soc* **2012,** *134* (45), 18503-18505.

16.   Liang, X. Y.; Parkinson, J. A.; Parsons, S.; Weishaupl, M.; Sadler, P. J., Cadmium cyclam complexes: Interconversion of cis and trans configurations and fixation of CO_2. *Inorg Chem* **2002,** *41* (17), 4539-4547.

17.   Freeman, G. M.; Barefield, E. K.; Vanderveer, D. G., Studies on Nickel(Ii) Complexes of Cyclam Ligands Containing Functionalized Nitrogen Substituents - Synthesis, Isomerization, and N-Dealkylation. *Inorg Chem* **1984,** *23* (20), 3092-3103.

18.   Maimon, E.; Zilbermann, I.; Cohen, H.; Kost, D.; van Eldik, R.; Meyerstein, D., Mechanism of isomerization of Ni(cyclam) in aqueous solutions. *Eur J Inorg Chem* **2005,** (24), 4997-5004.

19.   Piguet, C., Paramagnetic susceptibility by NMR: The ''solvent correction'' removed for large paramagnetic molecules. *J Chem Educ* **1997,** *74* (7), 815-816.

20.   Evans, D. F., The Determination of the Paramagnetic Susceptibility of Substances in Solution by Nuclear Magnetic Resonance. *J Chem Soc* **1959,** (Jun), 2003-2005.

21.   Bond, C. J.; Sokolow, G. E.; Crawley, M. R.; Burns, P. J.; Cox, J. M.; Mayilmurugan, R.; Morrow, J. R., Exploring Inner-Sphere Water Interactions of Fe(II) and Co(II) Complexes of 12-Membered Macrocycles To Develop CEST MRI Probes. *Inorg Chem* **2019,** *58* (13), 8710-8719.

22.   Olatunde, A. O.; Cox, J. M.; Daddario, M. D.; Spernyak, J. A.; Benedict, J. B.; Morrow, J. R., Seven-coordinate Co(II), Fe(II) and six-coordinate Ni(II) amide-appended macrocyclic complexes as ParaCEST agents in biological media. *Inorg Chem* **2014,** *53* (16), 8311-21.

23.   Randtke, E. A.; Chen, L. Q.; Corrales, L. R.; Pagel, M. D., The Hanes-Woolf linear QUESP method improves the measurements of fast chemical exchange rates with CEST MRI. *Magn Reson Med* **2014,** *71* (4), 1603-12.

24.   Woessner, D. E.; Zhang, S. R.; Merritt, M. E.; Sherry, A. D., Numerical solution of the Bloch equations provides insights into the optimum design of PARACEST agents for MRI. *Magn Reson Med* **2005,** *53* (4), 790-799.

25.   Sherry, A. D.; Wu, Y. K., The importance of water exchange rates in the design of responsive agents for MRI. *Curr Opin Chem Biol* **2013,** *17* (2), 167-174.

26.   Rancan, G.; Castelli, D. D.; Aime, S., MRI CEST at 1T With Large µ(eff) Ln(3+) Complexes Tm(3+)-HPDO3A: An Efficient MRI pH Reporter. *Magn Reson Med* **2016,** *75* (1), 329-336.

27.   Thorarinsdottir, A. E.; Tatro, S. M.; Harris, T. D., Electronic Effects of Ligand Substitution in a Family of Co-2(II) PARACEST pH Probes. *Inorg Chem* **2018,** *57* (17), 11252-11263.
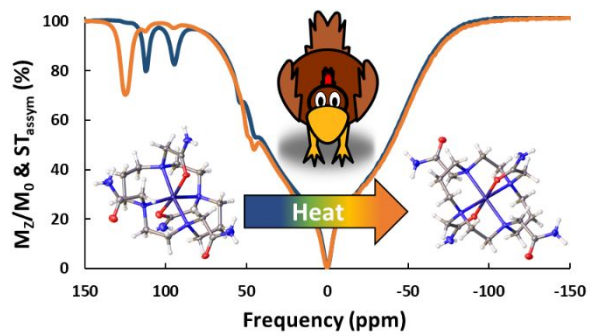
Two isomeric Co(II) paraCEST MRI probes produce a signal correlated to pH in solution and in tissue homogenate.